RESEARCH ARTICLE

Key Points:
- Survey of pickup ions at Titan using CAPS/IMS plasma data
- Signatures observed in the anti-Saturn side of the moon
- Mass loss of approximately 570 kg/d to 1 t/d estimated through freshly produced pickup ions of $m/q = 16$ to 28

Correspondence to:
L. H. Regoli,
leonardo.regoli.12@ucl.ac.uk

Survey of pickup ion signatures in the vicinity of Titan using CAPS/IMS

L. H. Regoli[1,2,3], A. J. Coates[1,2], M. F. Thomsen[4], G. H. Jones[1,2], E. Roussos[3], J. H. Waite[5], N. Krupp[3], and G. Cox[6,7]

[1]Mullard Space Science Laboratory, University College London, London, UK, [2]Centre for Planetary Sciences at UCL/Birkbeck, London, UK, [3]Max Planck Institute for Solar System Research, Göttingen, Germany, [4]Planetary Science Institute, Tucson, Arizona, USA, [5]Southwest Research Institute, San Antonio, Texas, USA, [6]School of Environmental Sciences, University of Liverpool, Liverpool, UK, [7]Department of Applied Mathematics, University of Leeds, Leeds, UK

Abstract Pickup ion detection at Titan is challenging because ion cyclotron waves are rarely detected in the vicinity of the moon. In this work, signatures left by freshly produced pickup heavy ions ($m/q \sim 16$ to $m/q \sim 28$) as detected in the plasma data by the Cassini Plasma Spectrometer/Ion Mass Spectrometer (CAPS/IMS) instrument on board Cassini are analyzed. In order to discern whether these correspond to ions of exospheric origin, one of the flybys during which the reported signatures were observed is investigated in detail. For this purpose, ion composition data from time-of-flight measurements and test particle simulations to constrain the ions' origin are used. After being validated, the detection method is applied to all the flybys for which the CAPS/IMS instrument gathered valid data, constraining the region around the moon where the signatures are observed. The results reveal an escape region located in the anti-Saturn direction as expected from the nominal corotation electric field direction. These findings provide new constraints for the area of freshly produced pickup ion escape, giving an approximate escape rate of $3.3^{+3}_{-2} \times 10^{23}$ ions· s^{-1}.

1. Introduction

After more than 110 dedicated flybys, the Cassini spacecraft has sampled the magnetospheric environment surrounding Titan, as well as its complex atmosphere and ionosphere, with both in situ and remote sensing measurements, providing an extensive data set to perform statistical studies of different aspects related to the moon-magnetosphere interaction.

Planetary bodies with atmospheres are constantly subjected to a variety of processes that contribute to the loss of atmospheric and ionospheric particles to surrounding space. The main processes causing atmospheric loss are the Jeans escape, which happens when atmospheric neutral particles are heated by external sources (e.g., solar radiation) until they reach a thermal velocity that surpasses the escape velocity, and the hydrodynamic escape, where the combination of heating from solar energy and upward thermal conduction leads to a constant outflow of neutrals [*Johnson et al.*, 2009].

At Titan, the Jeans parameter λ (the ratio between gravitational and thermal energy), which determines the escape process, is relatively large. As a consequence, Jeans escape is the predominant loss process for low mass ions (H_2), while for larger masses (CH_4 and N_2) sputtering or ionization and further ion pickup dominate. This was further confirmed in *Tucker and Johnson* [2009] by means of a direct simulation Monte Carlo description of the mass loss process.

Atmospheric escape rates of different species at Titan have been calculated by several authors. Good general reviews on the topic are available in *Johnson et al.* [2009] and *Strobel and Cui* [2014]. The H_2 escape rate was calculated separately by *Strobel* [2009] and *Cui et al.* [2011] with both obtaining identical results of $9.2 \times 10^{27} H_2 \cdot s^{-1}$. For the case of atomic H, *Hedelt et al.* [2010] estimated a Jeans escape rate of $1.74 \times 10^{27} H \cdot s^{-1}$ using a combination of data from the HDAC instrument from Cassini's T9 flyby and Monte Carlo simulations.

When it comes to neutral CH_4, an escape rate of $1.7 \times 10^{27} CH_4 \cdot s^{-1}$ was inferred by *Strobel* [2009] based on Ion and Neutral Mass Spectrometer (INMS) measurements and ionospheric chemistry models. However, an imbalance between the production and escape of CH_4 remains.

In terms of ionospheric escape, the main processes are field-aligned outflows and pickup ion escape. The first process, analogue to the polar wind observed in the Earth's magnetosphere, is driven by photoelectrons which move along the magnetic field and set up an ambipolar electric field that causes ions to escape [*Coates et al.*, 2015]. Pickup ion escape happens when a new ion with a relatively low thermal velocity is affected by local electromagnetic fields, accelerating it initially in the direction of the local electric field and subsequently producing a gyration around the magnetic field according to the Lorentz force. Pickup ions, apart from their contribution to ionospheric escape, have been also shown to play an important role when they reencounter the atmosphere inducing exospheric heating and further losses through atmospheric sputtering [*Tseng et al.*, 2008; *Michael et al.*, 2005].

For field-aligned outflows, *Coates et al.* [2012] looked at Cassini Plasma Spectrometer/Electron Spectrometer (CAPS/ELS) and CAPS/Ion Mass Spectrometer (IMS) data from the T9, T63, and T75 flybys (all distant tail encounters) and estimated total plasma loss rates of the order of 10^{24} ions $\cdot$ s^{-1}. When looking at different masses (specifically $m/q = 1 - 2$, $m/q = 16$, and $m/q = 28$), they reported consistently lower values for the low masses as well as variations between the different encounters. These differences could be due to real variations or uncertainties in the estimations.

Ion escape was also estimated by *Sittler et al.* [2010], using CAPS data for the T9 and T18 flybys, at $\sim 4 \times 10^{24}$ ions $\cdot$ s^{-1} and by *Wahlund et al.* [2005] using Langmuir probe data from the first two close flybys (TA and TB), estimating an ionospheric escape flux of 10^{25} ions $\cdot$ s^{-1}.

Given the dynamic nature of Titan's magnetospheric environment, the escape rates seem to vary according to factors such as the upstream plasma conditions. This was demonstrated using hybrid simulations by *Lipatov et al.* [2011] where the inclusion of O$^+$ in the background plasma helped them reproduce the ion densities observed during the T9 flyby.

More recently, *Woodson et al.* [2015] studied the composition of ions escaping from Titan using CAPS/IMS and INMS data from the T40 encounter, finding that the spectra are dominated by a light population, formed of H$^+$, H$_2^+$, and H$_3^+$ (being this the first detection of H$_3^+$ in Titan's exosphere), and two hydrocarbon groups.

The main focus of this paper is the ionospheric escape by freshly produced heavy ($m/q \sim 16$ to $m/q \sim 28$) pickup ions. Pickup ions are initially accelerated along the local electric field and, given that the electric field is nominally perpendicular to the magnetic field, the original population will have a narrow pitch angle (angle between the ion's parallel velocity and the local magnetic field direction) distribution centered at 90°, corresponding to a ring distribution in velocity space. This situation can differ when the field has a strong radial component while the corotating flow still dominates. In such conditions, freshly produced pickup ions can have an important field-aligned velocity component and the original pitch angle distribution will differ from the aforementioned ring distribution. These cases are not detectable with the analysis presented in this paper and are thus not considered.

The ring distribution is unstable to the creation of ion cyclotron waves (ICWs), one of the main footprints left by the creation of pickup ions that has been observed at different solar system bodies like comets [*Coates et al.*, 1990, 1993; *Coates and Jones*, 2009], Mars, and Venus [*Cravens et al.*, 2002; *Rahmati et al.*, 2015; *Grebowsky et al.*, 2004] as well as several moons in the Jovian [*Crary and Bagenal*, 2000; *Huddleston et al.*, 2000; *Volwerk et al.*, 2001] and Saturnian [*Teolis et al.*, 2010; *Tokar et al.*, 2008, 2012] systems.

At Titan, however, ICWs are rarely observed, with indications of their presence in only two of the more than a hundred flybys to date, namely T63 and T98 [*Russell et al.*, 2016]. *Cowee et al.* [2010] used 1-D simulations to study the growth of waves and attributed the lack of these to different causes like the fact that the ambient magnetic field at Titan's orbit is variable enough as to leave any ICW signature buried in the noise. Alternatively, the waves have a growth time that exceeds the convection time of the flux tubes crossing Titan's interaction region, making it impossible to detect them before they are diffused in the magnetospheric environment past the moon.

Even though ICWs are generally not observed, pickup ions also leave a clear signature in the ion data [*Hartle et al.*, 2006; *Coates*, 2009]. Additionally, while the magnetospheric plasma at Titan's orbit is mainly composed of H$^+$ H$_2^+$, and W$^+$ [*Thomsen et al.*, 2010], the ionospheric plasma outflow has high concentrations of H$_2^+$, CH$_4^+$, and N$_2^+$, as well as other chemical ion-neutral subproducts from the original ionization of molecular nitrogen and methane that have been detected escaping from the moon such as CH$_3^+$, CH$_4^+$, CH$_5^+$, HCNH$^+$, and C$_2$H$_5^+$, using both the Ion and Neutral Mass Spectrometer (INMS) [*Westlake et al.*, 2012] and CAPS/IMS
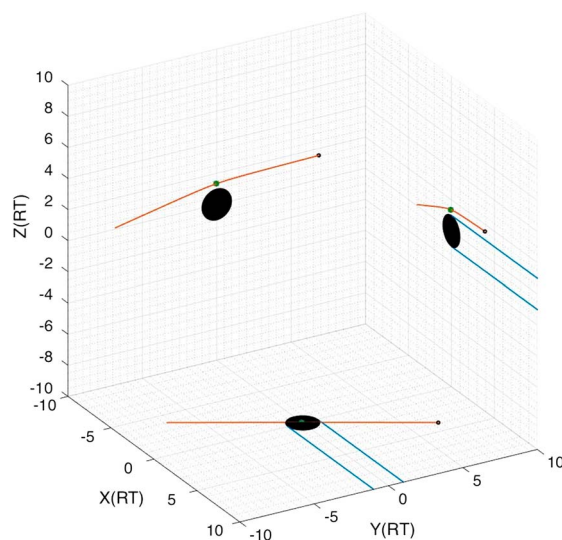
Figure 1. Cassini's trajectory during the T70 flyby. The plot is shown in TIIS coordinates with the *X* axis pointing toward the ideal corotation direction, the *Y* axis toward Saturn, and the *Z* axis completing the right-handed coordinate system. The green marker shows the moment of CA, and the black marker shows the starting point of the shown trajectory.

[*Sittler et al.*, 2010]. For this reason, analyzing the composition of the detected ions can provide a hint as to their origin as well.

The instability of the ring distribution mentioned above leads to the diffusion of the pitch angle distribution of the newly created ion population toward a shell distribution. Additionally, due to the energy lost to the waves, the energy of the original population will also get diffused, ending up, after a few gyrations, in a population much wider in energy as well. Since the gyrations undergone and the distance traveled from the position where the ions were created are directly related to the mass of the ions, the detection of pickup ions in the early phase of the pickup process, i.e., still on a ring distribution, is more likely for heavy species than for light ions.

In this paper, we provide a survey of pickup ion signatures detected by the CAPS/IMS instrument on board Cassini. We focus on the ions detected in the early stages of the pickup process by performing a systematic study of the observed signatures. We analyze in detail one of the flybys where the features of interest are observed to support the idea that those features correspond to freshly produced pickup ions. Based on that analysis, we identify the position with respect to the moon where similar signatures are observed during the different flybys. These locations are then presented on a Titan-centered map to define a region where heavy ions are flowing away from the moon.

Finally, the ion fluxes through three different planes with cross sections defined by the identified signatures are estimated based on the differential energy flux measurements provided by CAPS/IMS.

2. Data Set

In the present survey, ion data from the CAPS/IMS instrument on board Cassini are used in order to directly detect the presence of pickup ions by the characteristic signature they leave.

The survey is focused on the detection of pickup ions in the early stage of the pickup process, while they are still on a ring distribution in velocity space. The main signature of ions in this distribution is a narrow feature with pitch angles very close to 90°. These features are present in the plasma data and have been described and analyzed for the first Titan flyby (TA) by *Hartle et al.* [2006].

In this study, we looked at all the Titan flybys for which CAPS/IMS data are available. Unfortunately, the CAPS instrument was turned off in 2012 after the 83rd Titan flyby, but valid data for a total of 73 close flybys are available. For each of those flybys we searched for the same type of features reported by *Hartle et al.* [2006] in order to perform a statistical study of the frequency and location where these features are observed.
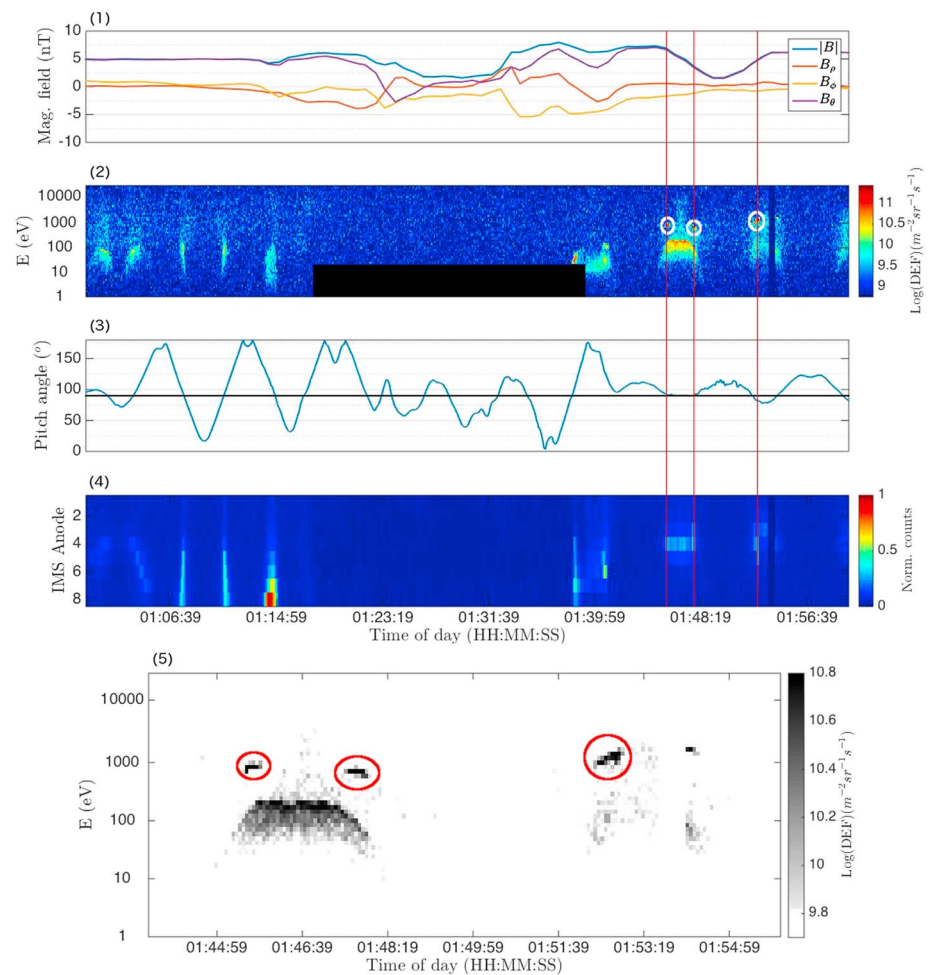
In order to validate our analysis and make sure that the signatures we study correspond to freshly produced pickup ions, we chose one specific flyby, namely T70, to perform a thorough analysis of the flyby data. T70 occurred on 21 June 2010 with closest approach (CA) happening at 01:27 UT at an altitude of 878.1 km. During the flyby, Cassini flew outbound (away from Saturn) from the plasma wake side of Titan toward the ram side over the north pole. The trajectory is shown in Titan interaction coordinate system (TIIS) in Figure 1.

The analysis performed for T70 is described in the next section and includes composition analysis based on coincident time of flight (TOF) measurements as well as a backtracing of ions on a background field from hybrid simulations in order to estimate the origin of the observed features.

Figure 2. Pickup ion signatures detected by CAPS/IMS during the T70 flyby. (first panel) Magnetic field data in Saturn-centered coordinates; (second panel) ion spectrogram for anode 4 with signatures left by freshly produced pickup ions encircled by white ovals; (third panel) instantaneous pitch angle detection for anode 4; (fourth panel) normalized counts for all the anodes; and (fifth panel) detail of the time where the signatures referred to are detected with signatures once again encircled by red ovals (the flux range and the colormap were changed to enhanced signatures of interest). Red vertical lines in Figure 2 (first to fourth panels) mark the pickup ion signatures with 90° pitch angle. For the region marked with a black rectangle in the low energies at the middle of Figure 2 (second panel), data are not collected to protect the instrument while traversing the ionosphere. The wavy structure of the spectrograms is an effect of the instrument's actuator [*Young et al.*, 2004].

For the rest of the flybys, the times when the signatures are observed and the corresponding location in space around Titan were recorded to provide a three-dimensional map of the positions where newly created ions are detected by Cassini.

3. Data Analysis

Figure 2 shows plasma data for the T70 flyby. Figure 2 (first panel) shows magnetic field data in Saturn-centered polar coordinates (ρ, θ, ϕ). Of all the Titan flybys to date, T70 was the only one with a magnetic field configuration similar to that observed by Voyager 1, with the field being mostly aligned with the planet's rotation axis pointing southward [*Simon et al.*, 2015].

Figure 2 (second and third panels) shows the energy spectrogram as detected by anode 4 and the instantaneous pitch angle coverage by the same anode, respectively. The narrow features highlighted with white circles are the ones left by freshly produced pickup ions. A detail of these features can be seen in Figure 2 (fifth panel), where the flux scale and colormap were changed in order to better highlight them (marked with red circles in this panel).
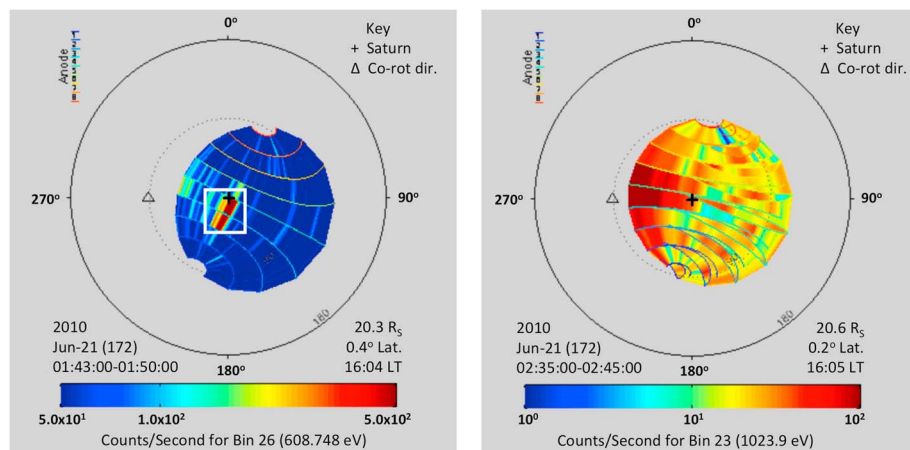
Figure 3. Angular distributions as captured by CAPS/IMS. The circle in the middle shows the field of view of the instrument with the plus sign marking the location of Saturn and the triangle the direction of ideal corotation. The plotted values in both panels reflect the counts at the peak energy of the distribution at the given time. (left) The distribution at the time where the signatures are detected (enmarked in white rectangle), showing a narrow distribution with pitch angle of 90° well away from the corotation direction. (right) The distribution upstream of the moon (after CA) showing a clear enhancement in the corotation direction.

The features are detected when the instrument is looking at pitch angles of 90° and have a very narrow energy distribution. This is because they are detected by the instrument within the first gyration or at least before they get scattered in the ambient plasma and thus still have a beam-like distribution.

Figure 2 (fourth panel) shows normalized counts detected by each one of the eight CAPS/IMS anodes. To get these normalized counts, for each individual measurement (timeslice), the maximum value of all the anodes is taken, and all the values are divided by the absolute maximum of the whole time covered. This is a similar plot to the one presented by *Wilson et al.* [2010] using CAPS data near Rhea and, even though the electromagnetic environment at Titan is much more complex than at Rhea, outside the interaction region this plot gives an idea of the direction where the flow is coming from.

By looking at the normalized counts in Figure 2, we may infer that the corotating flow was not in the field of view of CAPS/IMS during the interval where the sample was taken. This is because the signal is rather weak in all anodes during the whole time, except for some enhancement present between ∼01:35:00 and ∼01:55:00, right after CA. These enhancements correspond to the signals interpreted as pickup ions.

There is also a much wider distribution before CA (between 01:00:03 and ∼01:16:00) that seems to peak outside anode 8. This wider distribution suggests a magnetospheric origin, so it can be seen that the signatures detected are actually coming from somewhere else.

The distinction between the origin of the signatures and the corotation direction is also visible in Figure 3 where angular distributions of the ion populations captured by CAPS/IMS for two different times are shown (left during the time of the detection and right after leaving the interaction region, in the upstream magnetospheric flow). The pickup ion signatures are marked in Figure 3 (left) with a white square.

The CAPS/IMS analyzer has an intrinsic energy resolution of $\Delta E/E = 0.17$. The fact that the signal in the bins adjacent to the peak channel in Figure 2 is at about 1 order of magnitude lower than the peak indicates that the distribution of the detected ion population is relatively narrow, with a thermal spread of $<\sim170$ eV. Such a narrow distribution, also visible in the spectrum shown in Figure 4, is strong evidence that these ions are of local origin.

Another indication that the population might correspond to freshly produced pickup ions is that their pitch angle is rather narrowly confined to 90°, something expected for pickup ions relatively close to the source (within the first gyration after being picked up). Since the electromagnetic environment at Titan is quite variable [*Backes et al.*, 2005; *Bertucci et al.*, 2007; *Simon et al.*, 2015], it is expected that the distribution will change fairly fast once the ions drift away from the region where they were created.
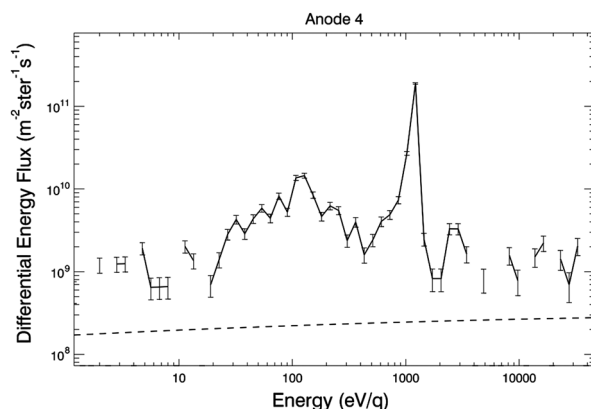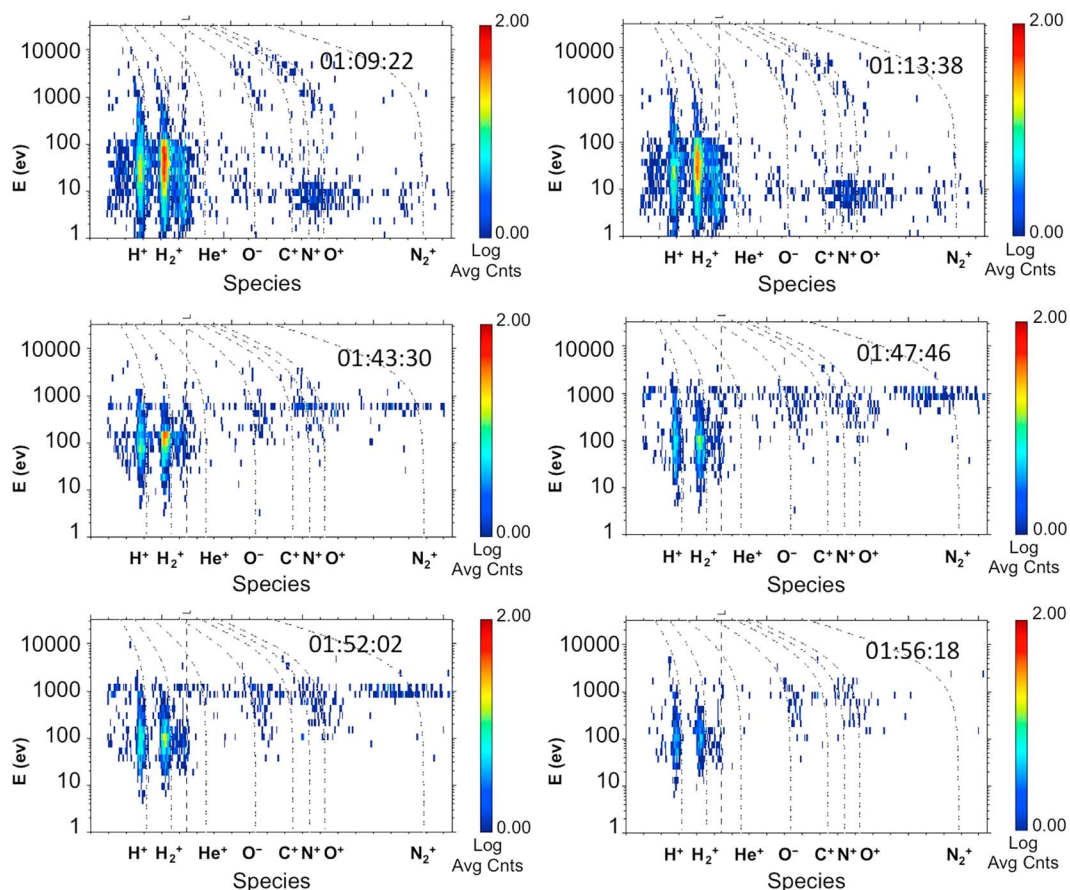
Figure 4. Differential energy flux (DEF) spectrum for anode 4 during the detection of one of the features hereby interpreted as freshly produced pickup ions.

At Titan's orbit, due to the centrifugal forces imposed by the fast rotation of the planet, it is expected that the magnetospheric plasma will have pitch angles close to 90° as well. For this reason, it is important to rule out that at the moment of the detection, CAPS/IMS is not detecting background plasma from Saturn's magnetosphere.

A further analysis to determine whether the ions originate near the moon or at the magnetosphere involves examining the plasma composition from the TOF data. Figure 5 shows composition information for different periods before and after CA. The region in between is excluded from the analysis since Cassini flew through the ionosphere where pickup ions would not be present. For each panel, the time shown corresponds to the beginning of a 4 min integration.

As mentioned before, the magnetospheric plasma at Titan's orbit (20 R_S) is mainly composed of H$^+$ ($m/q = 1$), H$_2^+$ ($m/q = 2$), and W$^+$ ($m/q \sim 16$) [*Thomsen et al.*, 2010]. The fluxes will depend on the position at a given time

Figure 5. Ion composition obtained from time-of-flight (TOF) analysis with integration time of 4 m and 16 s (times shown correspond to start of integration). (top row) The data obtained before CA but already within Titan's interaction region, where enhancements on $m/q = 2$, $m/q = 16$, and $m/q = 28$ populations are visible. (second row and bottom left) Data obtained during the time when the pickup ion signatures were observed. (bottom right) Data from a time after CA when Cassini was already upstream of the moon.
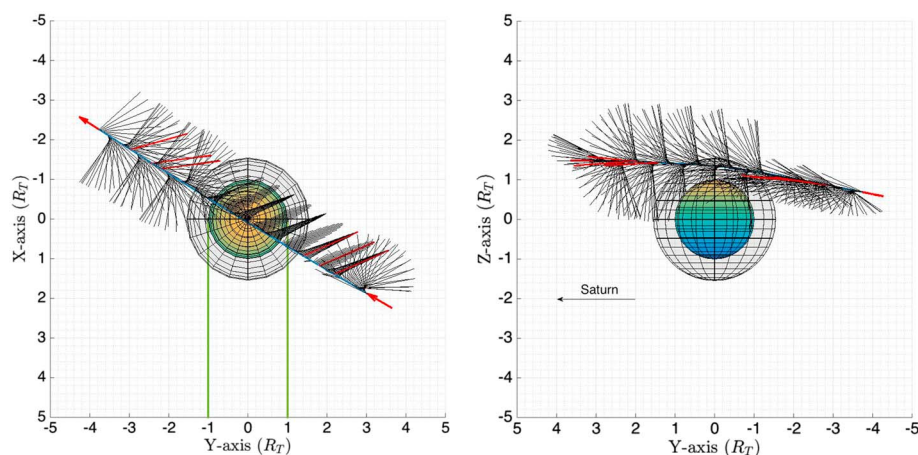
Figure 6. Cassini's trajectory during the T70 flyby with the instantaneous CAPS/IMS look direction overplotted (black lines). The red arrows at the beginning and the end of the trajectory indicate the direction of travel, and the seven thick red lines (three before CA and four after CA) show the locations where signatures with 90° pitch angle are observed. The three detections after CA are the ones interpreted as freshly produced pickup ions.

of the magnetospheric current sheet with respect to the equatorial plane, given the change in shape that the current sheet undergoes due to the interaction of the planet's magnetic field with the solar wind [*Arridge et al.*, 2011]. Additionally, the detected fluxes will vary according to the angle between corotation direction and the instrument's look direction.

From Figure 5 it can be seen that as Cassini approaches Titan, an enhancement in $m/q \sim 16$ ions with low energy (around 10 eV, likely field-aligned outflows) is present (before CA). Once Cassini leaves the ionosphere, an enhancement in higher energy $m/q \sim 16$ ions (around 1 keV) as well as close to $m/q \sim 28$ ions (again at 1 keV) occurs. It is beyond the scope of this study to identify the actual composition of these ions, but this enhancement could be due to any of the ions reported in the literature, such as CH_3^+, CH_4^+, or CH_5^+ for $m/q \sim 16$ or $HCNH^+$ for $m/q \sim 28$ [*Westlake et al.*, 2012; *Sittler et al.*, 2010]. A detailed explanation of the TOF measurements and the ion species determination using CAPS can be found in *Thomsen et al.* [2014].

What is clear throughout the whole period analyzed except for the last panel (Figure 5, bottom right, at 01:56:18) is that there was an enhancement of $m/q = 2$ with respect to $m/q = 1$. This is also interpreted as H_2^+ being picked up from the moon and directed by the local electromagnetic field toward Cassini, something that was first reported in *Sittler et al.* [2010]. These ions leave a signature much wider in pitch angle and energy than heavy ions since by the time they reach the instrument, they have undergone many gyrations due to their lower mass and consequently smaller gyroradius.

In Figure 5, the three panels obtained at 01:43:30, 01:47:46, and 01:52:02 are coincident with the time of the detections being analyzed here. It can be seen that at approximately 1 keV (the same energy of the features shown in Figure 2) an enhancement on the $m/q \sim 16$ to $m/q \sim 28$ can be observed. This observation, combined with the narrow distribution already shown, is an indication of the presence of heavy pickup ions being detected by the instrument.

The enhancement in the channel corresponding to O^-, corresponding to negative oxygen ions produced at the carbon foil [*Thomsen et al.*, 2010], is an indication that the $m/q \sim 16$ detection corresponds to a mixture of both ionospheric (possibly CH_4) and magnetospheric (O^+) origin.

Figure 6 shows Cassini's trajectory during the flyby with the look direction of CAPS/IMS overplotted. The three thick red lines before CA mark the location, where the signatures with wide energy distribution and 90° pitch angle are detected. The three thick red lines after CA mark the locations where the freshly produced pickup ions are observed.

Notice that the look direction of the instrument after CA matches that expected for the detection of exospheric ions being picked up along the direction of the ideal corotation electric field, whereas the look direction before CA corresponds to that expected for the detection of magnetospheric ions or, as stated above, field-aligned outflows that are able to reach that location due to local electromagnetic disturbances.
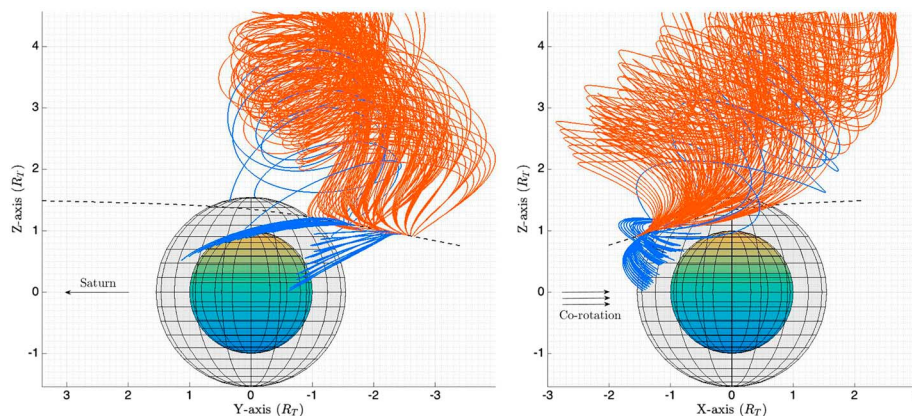
Figure 7. Ion trajectories backtraced from the instrument's position during the time when the two signatures around 1:46:43 in Figure 2 are observed. The ions simulated are $m/q = 16$. The sphere at the center represents Titan with the spherical mesh representing the location of the moon's exobase (1450 km above the surface). The dashed line shows the trajectory of Cassini during the flyby, the orange lines represent trajectories that map back to the magnetosphere while the blue ones represent trajectories of ions that seem to be coming from the exosphere. The ions were simulated with an energy range from 500 eV to 1 keV, and the background fields were obtained from an A.I.K.E.F. hybrid simulation. Both figures are in TIIS coordinates with the left one showing the trailing hemisphere and the right one the anti-Saturn side.

A final analysis to better constrain the origin of the ions consists of a test particle simulation to backtrace ions from the instrument with a background field to confirm whether they come from the magnetosphere or from the exosphere. For this, the same tracing software package used in *Regoli et al.* [2015] was used with the electromagnetic field configuration for T70 obtained from a hybrid simulation (kinetic ions and fluid electrons) using the A.I.K.E.F. code [*Müller et al.*, 2011].

For the simulation, the time surrounding the first two signatures encircled in white in Figure 2, specifically from 01:40:00 to 01:50:00, was considered. Single charged ions with $m = 16$ and energies from 500 eV to 1 keV were backtraced from the position and into the look direction of the instrument. For the tracing, the elevation and azimuth fields of view of the instrument were taken into account. Figure 7 shows the results of the simulation. The fact that some of the trajectories seem to coincide with ions coming from the exosphere and reaching the instrument within their first gyration further confirms that the signatures observed could be produced by ions coming from the moon.

Since no information on the upstream composition is given as an input for the backtracing simulations, the results can only be interpreted in connection with the other analyses presented in this section. The fact that some of the ions simulated originate from the magnetosphere does not mean that ions with $m = 16$ are indeed coming from the magnetosphere. The simulations can only tell that, given the electromagnetic field configuration observed during the T70 flyby, if a population of heavy ions were present in the magnetosphere, these could indeed reach the instrument at the simulated time period.

In general, these results are in agreement with observations already made during the Voyager 1 flyby as reported by *Sittler et al.* [2005]. Analyzing the spectra from the PLS instrument, they found that finite gyroradius effects are dominant in the interaction of Titan with the corotating magnetospheric plasma.

4. Outflow Region and Estimated Escape

During 27 of the 73 analyzed flybys, pickup ion signatures with the expected narrow pitch angle distribution, i.e., captured in an early phase of the ring distribution, were observed. The locations with respect to Titan are indicated in Figure 8.

From Figure 8 it is obvious that the pickup ion signatures are consistently observed on the anti-Saturn side. Given that the nominal corotation electric field points away from Saturn and that the ideal corotation direction is a good approximation as reported by *Arridge et al.* [2011], the fact that the signatures are observed in the anti-Saturn side of the moon is an additional confirmation that they correspond to freshly produced pickup ions.
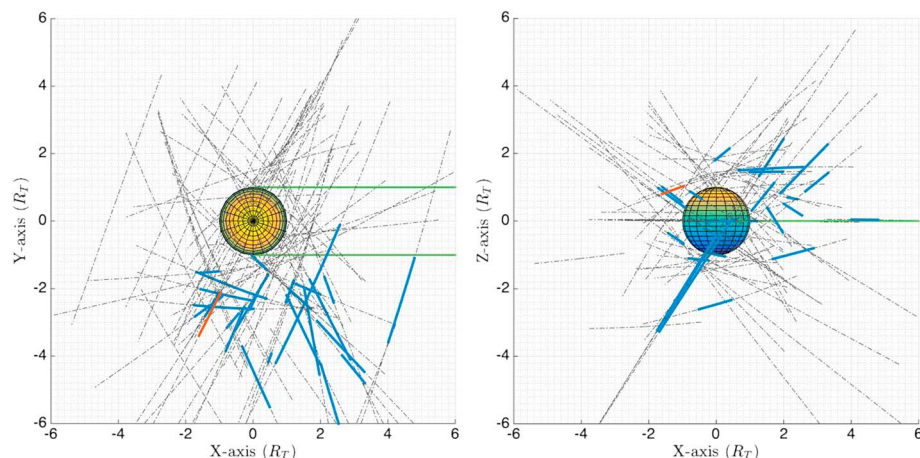
Figure 8. Location of pickup ion signatures observed by CAPS/IMS. Titan is the sphere in the center with the spherical transparent grid representing the exobase; all the flyby trajectories (up to T83) are represented by dashed lines, and the blue regions are where the signatures were observed. T70 is marked with a red line. The parallel green lines show the ideal corotation direction. The plot is shown in TIIS coordinates with an (left) equatorial projection and a (right) side view from the anti-Saturn side.

The detection of signatures outside the equatorial plane as observed in Figure 8 (right) arises both from detection of pickup ions originating from high latitudes but also from the fact that the magnetic field during many of the flybys has also a nonnegligible θ component, meaning that the electric field can also have a component pointing away from the equatorial plane.

By taking three different planes along the X direction limited by the regions where signatures are observed as representative of the region where freshly produced pickup ions escape, we are able to give an estimate of the contribution to the atmospheric escape from the observed species. We do this by integrating the differential energy flux (DEF) for the signatures of interest taking into account the angular distribution shown in Figure 3 (left). The enhancement is constrained to $\sim$40° in elevation (two adjacent anodes) by $\sim$20° in azimuth (which is related to the instantaneous pitch angle coverage of a given anode). This corresponds to a solid angle of $\sim$0.24 sr.

Even though the width of the signature may present variations from one detection to the other, the fact that the detections are always at a pitch angle of 90° and that they are always constrained to one to two adjacent anodes sets this solid angle value as an upper limit for the distribution. For this reason, a solid angle of $\sim$0.24 sr is used for all the detections.

The DEF is calculated from the counts detected by the instrument according to equation (1), where C_{Accum} are the counts detected by the instrument during an integration time (dt), SF is a scale factor that takes into account the microchannel plate gain, and G is the geometric factor of the instrument in $m^{-2} \cdot sr^{-1} \cdot eV/eV$, which is dependent on the anode and the energy step.

$$DEF = \frac{C_{Accum}}{(dt)(SF)(G)} \qquad (1)$$

The fact that the geometric factor of the instrument already includes the energy step of each channel implies that the integration is made by simply adding the fluxes detected at the energy bins where the enhancement is observed. Given the narrow distribution in energy of the features being considered in this study, only the flux at the peak energy is considered since the adjacent bins present fluxes that are at least 1 order of magnitude lower (Figure 4).

We took different planes to compare the escape rates at different locations. The planes are parallel to the Y-Z plane at $X = 1$, $X = 1.6$, and $X = 2.4$ and contain the signatures of the ions that are observed downstream of the moon, even though still on the anti-Saturn side. For the escape calculations an average of the fluxes from the flybys that crossed a specific plane was taken and integrated all over the area of that plane. For each flyby, the mean value of all the detections made during that flyby is used.
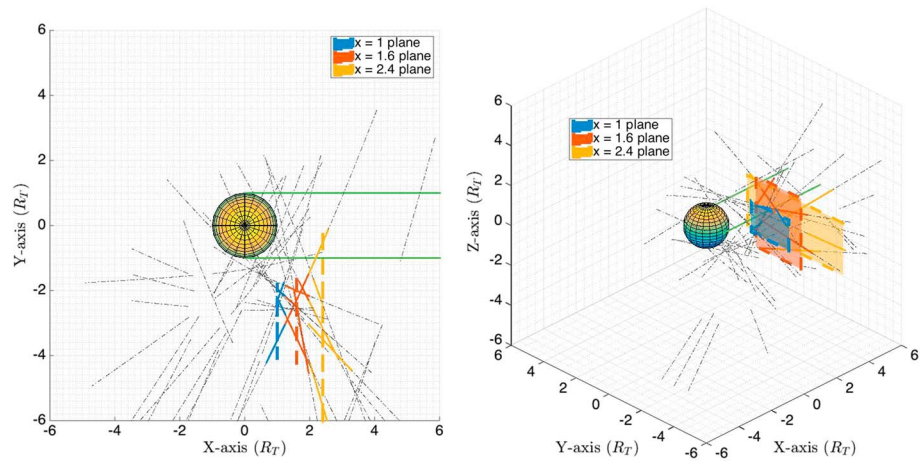
Figure 9. (left) Polar and (right) three-dimensional view of the three planes used to calculate the pickup ion fluxes as described in the text. The flybys contributing to the calculation of each plane are depicted by lines with the same color as the corresponding planes. The flybys that do not contribute to the calculations are shown with dashed lines.

Figure 9 shows a polar (left) and a 3-D (right) view of the three planes used with the flybys color coded according to the plane to which they contribute. For flybys contributing to more than one plane, different sections of the trajectory are colored according to the plane they cross at a given sector.

The cross sections of the planes can serve as an estimate of the region where ions escape, even though given the low number of samples available, these cannot be taken as an accurate estimate. However, and as expected, the cross section of the parallel planes on the X direction grows with the distance from the moon, something caused by the widening of the tail region with distance as simulations indicate.

The areas in R_T^2 for each plane are 3.56 ($X = 1$), 5.68 ($X = 1.6$), and 18.9 ($X = 2.4$). The fact that the areas grow with increasing distance from the moon is consistent with ions propagating outward in different directions. The coordinates of the corners of each plane as well as the corresponding areas are listed in Table 1.

In terms of DEF, for the first plane ($X = 1$), with five data points (T11, T16, T55, T57, and T63), the median of the values measured was 8.6×10^{10} m$^{-2} \cdot$ sr$^{-1} \cdot$ s^{-1}. For the second plane ($X = 1.6$), with five data points (TA, T16, T55, T57, and T63), the median was 1.5×10^{11}. Finally, for the third plane ($X = 8.3$), with four data points (TB, T3, T62, and T63), the median was 1.3×10^{11}.

For each of the three planes ($X = 1$, $X = 1.6$, and $X = 2.4$), the estimated ion outflow was, respectively, 8.3×10^{22} ions$\cdot$ s^{-1}, 2.4×10^{23} ions$\cdot$ s^{-1}, and 4.2×10^{23} ions$\cdot$ s^{-1}. Taking the average of the individual fluxes, an estimate of $3.3^{+3}_{-2} \times 10^{23}$ ions$\cdot$ s^{-1} was obtained. A summary of all these values and the corresponding errors is shown in Table 2.

Using an expression for the phase space density derived from the Vlasov equation, *Hartle and Sittler* [2007] showed that the ratio between the gyroradius of an ion component and the scale height ($\alpha = r_g / H$) is a crucial factor determining the type of interaction. If $\alpha << 1$ the interaction is fluid like while for $\alpha >> 1$ the pickup ions are detected as beams, as the ones reported in this study.

They also found that the pickup ion density increases with decreasing values of α due to more sources contributing to the detection location. The differences between the three planes might be a result of this

Table 1. Coordinates of Corners and Areas of Planes Used to Calculate Fluxes[a]

Plane	Corner 1	Corner 2	Corner 3	Corner 4	Area
$X = 1$	(1.00, −4.08, 0.00)	(1.00, −4.08, 1.53)	(1.00, −1.75, 1.53)	(1.00, −1.75, 0.00)	3.56
$X = 1.6$	(1.60, −3.63, −1.11)	(1.60, −3.63, 1.88)	(1.60, −1.73, 1.88)	(1.60, −1.73, −1.11)	5.68
$X = 2.4$	(2.40, −7.82, −0.94)	(2.40, −7.82, 1.59)	(2.40, −0.37, 1.59)	(2.40, −0.37, −0.94)	18.9

[a]The coordinates are given as (X,Y,Z) vectors in units of R_T. The areas are given in units of R_T^2.

Table 2. Median and Deviations From Differential Energy Flux (DEF) Measurements (in $m^{-2} \cdot sr^{-1} \cdot s^{-1}$) and Particle Fluxes (in ions $\cdot s^{-1}$)

Plane	DEF	Particle Flux
$X = 1$	$8.6 \pm 0.2 \times 10^{10}$	$8.3 \pm 0.2 \times 10^{22}$
$X = 1.6$	$1.5 \pm 0.03 \times 10^{11}$	$2.4 \pm 0.04 \times 10^{23}$
$X = 2.4$	$8.3 \pm 0.2 \times 10^{10}$	$4.2 \pm 0.1 \times 10^{23}$

dependence, but due to the relatively low statistics, with only four or five flybys crossing each plane, this cannot be definitely assessed.

5. Discussion and Conclusions

By combining data analysis and test particle simulations for the study of the narrow signatures recorded by the CAPS/IMS instrument when close to Titan, we were able to support the interpretation made by *Hartle et al.* [2006] that those signatures correspond to freshly produced pickup ions. We combined a composition analysis with test particle simulations to conclude that the ions generating the signatures indeed come from the moon's exosphere.

Then, by performing a survey of the signatures for all the flybys with good thermal ion data from CAPS/IMS, we calculated cross sections for three planes located at three positions on the anti-Saturn side downstream of the moon. The cross sections were constrained based on where the signatures are observed. The fact that all the observed signatures are on the anti-Saturn side, consistent with the ideal corotation electric field direction, further supports the original assumption of the signatures corresponding to freshly produced pickup ions.

Finally, calculating the particle fluxes through those three planes by integrating the DEF for the times where the signatures are observed, we were able to give an estimate of the ion outflow by pickup ions with mass between $m/q = 16$ and $m/q = 28$ of $3.3^{+3}_{-2} \times 10^{23}$ ions $\cdot s^{-1}$. This is a small fraction of the bulk ionospheric outflow estimated with midrange and distant tail measurements [*Coates et al.*, 2012; *Sittler et al.*, 2010], something expected since those studies take into account all the species escaping from the moon.

In terms of mass, this number corresponds to a loss of around 570 kg/d if only $m/q = 16$ is considered (lower limit) and of 1 t/d if only $m/q = 28$ is considered (upper limit). The mass-separated results obtained by *Coates et al.* [2012] are on the order of 7 t/d. This shows, in general, that the pickup process, although significant at around 8% to 15% of the total loss estimated on the tail (for the lower and upper limit values obtained, respectively), is unable to give a hint on the methane problem, namely the observed imbalance between the production and loss rates, that still remains.

References

Arridge, C. S., et al. (2011), Upstream of Saturn and Titan, *Space Sci. Rev.*, *162*, 25–83.

Backes, H., et al. (2005), Titan's magnetic field signature during the first Cassini encounter, *Science*, *308*, 992–995.

Bertucci, C., F. M. Neubauer, K. Szego, J.-E. Wahlund, A. J. Coates, M. K. Dougherty, D. T. Young, and W. S. Kurth (2007), Structure of Titan's mid-range magnetic tail: Cassini magnetometer observations during the T9 flyby, *Geophys. Res. Lett.*, *34*, L24S02, doi:10.1029/2007GL030865.

Coates, A. J. (2009), Interaction of Titan's ionosphere with Saturn's magnetosphere, *Philos. Trans. R. Soc. A*, *367*(1889), 773–788, doi:10.1098/rsta.2008.0248.

Coates, A. J., and G. H. Jones (2009), Plasma environment of Jupiter family comets, *Planet. Space Sci.*, *57*(10), 1175–1191, doi:10.1016/j.pss.2009.04.009.

Coates, A. J., B. Wilken, A. D. Johnstone, K. Jockers, K.-H. Glassmeier, and D. E. Huddleston (1990), Bulk properties and velocity distributions of water group ions at Comet Halley: Giotto measurements, *J. Geophys. Res.*, *95*(A7), 10,249–10,260, doi:10.1029/JA095iA07p10249.

Coates, A. J., A. D. Johnstone, B. Wilken, and F. M. Neubauer (1993), Velocity space diffusion and nongyrotropy of pickup water group ions at comet Grigg-Skjellerup, *J. Geophys. Res.*, *98*(A12), 20,985–20,994, doi:10.1029/93JA02535.

Coates, A. J., et al. (2012), Cassini in Titan's tail: CAPS observations of plasma escape, *J. Geophys. Res.*, *117*, A05324, doi:10.1029/2012JA017595.

Coates, A. J., A. Wellbrock, J. H. Waite, and G. H. Jones (2015), A new upper limit to the field-aligned potential near Titan, *Geophys. Res. Lett.*, *42*, 4676–4684, doi:10.1002/2015GL064474.

Cowee, M. M., S. P. Gary, H. Y. Wei, R. L. Tokar, and C. T. Russell (2010), An explanation for the lack of ion cyclotron wave generation by pickup ions at Titan: 1-D hybrid simulation results, *J. Geophys. Res.*, *115*, A10224, doi:10.1029/2010JA015769.

Crary, F. J., and F. Bagenal (2000), Ion cyclotron waves, pickup ions, and Io's neutral exosphere, *J. Geophys. Res.*, *105*(A11), 25,379–25,389, doi:10.1029/2000JA000055.

Cravens, T. E., A. Hoppe, S. A. Ledvina, and S. McKenna-Lawlor (2002), Pickup ions near Mars associated with escaping oxygen atoms, *J. Geophys. Res.*, *107*(A8), 1170, doi:10.1029/2001JA000125.

Cui, J., R. V. Yelle, I. C. F. Müller-Wodarg, and P. P. Lavvas (2011), The implications of the H2 variability in Titan's exosphere, *J. Geophys. Res.*, *116*, A11324, doi:10.1029/2011JA016808.

Grebowsky, J. M., D. H. Crider, D. S. Intriligator, R. E. Hartle, and M. H. Acuña (2004), Venus/Mars pickup ions and ionosheath wave structures, *Adv. Space Res.*, *33*(2), 176–181, doi:10.1016/j.asr.2003.04.014.

Hartle, R. E., and E. C. Sittler (2007), Pickup ion phase space distributions: Effects of atmospheric spatial gradients, *J. Geophys. Res.*, *112*, A07104, doi:10.1029/2006JA012157.

Hartle, R. E., et al. (2006), Preliminary interpretation of Titan plasma interaction as observed by the Cassini Plasma Spectrometer: Comparisons with Voyager 1, *Geophys. Res. Lett.*, *33*, L08201, doi:10.1029/2005GL024817.

Hedelt, P., Y. Ito, H. U. Keller, R. Reulker, P. Wurz, H. Lammer, H. Rauer, and L. Esposito (2010), Titan's atomic hydrogen corona, *Icarus*, *210*(1), 424–435, doi:10.1016/j.icarus,2010.06.012.

Huddleston, D. E., R. J. Strangeway, X. Blanco-Cano, C. T. Russell, M. G. Kivelson, and K. K. Khurana (2000), Io-Jupiter interaction: Waves generated by pickup ions, *Adv. Space Res.*, *26*(10), 1513–1518, doi:10.1016/S0273-1177(00)00091-0.

Johnson, R. E., O. J. Tucker, M. Michael, E. C. Sittler, H. T. Smith, D. T. Young, and J. H. Waite (2009), Mass loss processes in Titan's upper atmosphere, in *Titan from Cassini-Huygens*, edited by R. H. Brown, J.-P. Lebreton, and J. H. Waite, chap. 15, pp. 373–391, Springer, Netherlands.

Lipatov, A. S., E. C. Sittler, R. E. Hartle, J. F. Cooper, and D. G. Simpson (2011), Background and pickup ion velocity distribution dynamics in Titan's plasma environment: 3D hybrid simulation and comparison with CAPS T9 observations, *Adv. Space Res.*, *48*(6), 1114–1125, doi:10.1016/j.asr.2011.05.026.

Michael, M., R. E. Johnson, F. Leblanc, M. Liu, J. G. Luhmann, and V. I. Shematovich (2005), Ejection of nitrogen from Titan's atmosphere by magnetospheric ions and pick-up ions, *Icarus*, *175*(1), 263–267, doi:10.1016/j.icarus.2004.11.004.

Müller, J., S. Simon, U. Motschmann, J. Schüle, K.-H. Glassmeier, and G. J. Pringle (2011), A.I.K.E.F.: Adaptive hybrid model for space plasma simulations, *Comput. Phys. Commun.*, *182*, 946–966.

Rahmati, A., D. E. Larson, T. E. Cravens, R. J. Lillis, P. A. Dunn, J. S. Halekas, J. E. Connerney, F. G. Eparvier, E. M. B. Thiemann, and B. M. Jakosky (2015), MAVEN insights into oxygen pickup ions at Mars, *Geophys. Res. Lett.*, *42*, 8870–8876, doi:10.1002/2015GL065262.

Regoli, L. H., E. Roussos, M. Feyerabend, G. H. Jones, N. Krupp, A. J. Coates, S. Simon, U. Motschmann, and M. K. Dougherty (2015), Access of energetic particles to Titan's exobase: A study of Cassini's T9 flyby, *Planet. Space Sci.*, *130*, 40–53, doi:10.1016/j.pss.2015.11.013.

Russell, C. T., H. Y. Wei, M. M. Cowee, F. M. Neubauer, and M. K. Dougherty (2016), Ion cyclotron waves at Titan, *J. Geophys. Res. Space Physics*, *121*, 2095–2103, doi:10.1002/2015JA022293.

Simon, S., E. Roussos, and C. S. Paty (2015), The interaction between Saturn's moons and their plasma environments, *Phys. Rep.*, *602*, 1–65, doi:10.1016/j.physrep.2015.09.005.

Sittler, E. C., R. E. Hartle, A. F. Viñas, R. E. Johnson, H. T. Smith, and I. Mueller-Wodarg (2005), Titan interaction with Saturn's magnetosphere: Voyager 1 results revisited, *J. Geophys. Res.*, *110*, A09302, doi:10.1029/2004JA010759.

Sittler, E. C., et al. (2010), Saturn's magnetospheric interaction with Titan as defined by Cassini encounters T9 and T18: New results, *Planet. Space Sci.*, *58*, 327–350, doi:10.1016/j.pss.2009.09.017.

Strobel, D. F. (2009), Titan's hydrodynamically escaping atmosphere: Escape rates and the structure of the exobase region, *Icarus*, *202*(2), 632–641, doi:10.1016/j.icarus.2009.03.007.

Strobel, D. F., and J. Cui (2014), Titan's upper atmosphere/exosphere, escape processes, and rates, in *Titan: Interior, Surface, Atmosphere, and Space Environment*, edited by I. Müller-Wodarg et al., chap. 10, pp. 355–375, Cambridge Univ. Press, Cambridge, U. K., doi:10.1017/CBO9780511667398.013.

Teolis, B. D., et al. (2010), Cassini finds an oxygen–carbon dioxide atmosphere at Saturn's icy moon Rhea, *Science*, *330*(6012), 1813–1815, doi:10.1126/science.1198366.

Thomsen, M. F., D. B. Reisenfeld, D. M. Delapp, R. L. Tokar, D. T. Young, F. J. Crary, E. C. Sittler, M. A. McGraw, and J. D. Williams (2010), Survey of ion plasma parameters in Saturn's magnetosphere, *J. Geophys. Res.*, *115*, A10220, doi:10.1029/2010JA015267.

Thomsen, M. F., et al. (2014), Ion composition in interchange injection events in Saturn's magnetosphere, *J. Geophys. Res. Space Physics*, *119*, 9761–9772, doi:10.1002/2014JA020489.

Tokar, R. L., et al. (2008), Cassini detection of water-group pick-up ions in the Enceladus torus, *Geophys. Res. Lett.*, *35*, L14202, doi:10.1029/2008GL034749.

Tokar, R. L., R. E. Johnson, M. F. Thomsen, E. C. Sittler, A. J. Coates, R. J. Wilson, F. J. Crary, D. T. Young, and G. H. Jones (2012), Detection of exospheric O2+ at Saturn's moon Dione, *Geophys. Res. Lett.*, *39*, L03105, doi:10.1029/2011GL050452.

Tseng, W.-L., W.-H. Ip, and A. Kopp (2008), Exospheric heating by pickup ions at Titan, *Adv. Space Res.*, *42*, 54–60, doi:10.1016/j.asr.2008.03.009.

Tucker, O. J., and R. E. Johnson (2009), Thermally driven atmospheric escape: Monte Carlo simulations for Titan's atmosphere, *Planet. Space Sci.*, *57*(14–15), 1889–1894, doi:10.1016/j.pss.2009.06.003.

Volwerk, M., M. G. Kivelson, and K. K. Khurana (2001), Wave activity in Europa's wake: Implications for ion pickup, *J. Geophys. Res.*, *106*(A11), 26,033–26,048, doi:10.1029/2000JA000347.

Wahlund, J.-E., et al. (2005), Cassini measurements of cold plasma in the ionosphere of Titan, *Science*, *308*(5724), 986–989, doi:10.1126/science.1109807.

Westlake, J. H., et al. (2012), The observed composition of ions outflowing from Titan, *Geophys. Res. Lett.*, *39*, L19104, doi:10.1029/2012GL053079.

Wilson, R. J., R. L. Tokar, W. S. Kurth, and A. M. Persoon (2010), Properties of the thermal ion plasma near Rhea as measured by the Cassini plasma spectrometer, *J. Geophys. Res.*, *115*, A05201, doi:10.1029/2009JA014679.

Woodson, A. K., H. T. Smith, F. J. Crary, and R. E. Johnson (2015), Ion composition in Titan's exosphere via the Cassini Plasma Spectrometer I: T40 encounter, *J. Geophys. Res. Space Physics*, *120*, 212–234, doi:10.1002/2014JA020499.

Young, D. T., et al. (2004), Cassini plasma spectrometer investigation, *Space Sci. Rev.*, *114*, 1–112.